

<sup>74</sup>Ge( $\alpha,\alpha 3n\gamma$ ) 2022Wa21

Type	Author	Citation	Literature Cutoff Date
Full Evaluation	Balraj Singh and Jun Chen	NDS 188,1 (2023)	17-Jan-2023

**2022Wa21:** E( $\alpha$ )=58.6 and 62.6 MeV. Target=2.85 mg/cm<sup>2</sup> <sup>74</sup>Ge with a 10.8 mg/cm<sup>2</sup> backing. Measured E $\gamma$ , I $\gamma$ ,  $\gamma\gamma$ -coin,  $\gamma\gamma(\theta)$ (ADO),  $\gamma\gamma$ (linear pol) using the AFRODITE array with eight Compton-suppressed clover detectors and two low-energy photon spectrometers (LEPS detectors) at the Separated Sector Cyclotron facility of iThemba LABS. Deduced high-spin levels, J $\pi$ , bands, evidence for an octupole band from B(E1)/B(E2) ratios.

Detailed numerical data for E $\gamma$ , I $\gamma$ ,  $\gamma\gamma$ -coin,  $\gamma\gamma(\theta)$ (ADO),  $\gamma\gamma$ (linear polarization) were provided by the corresponding authors of **2022Wa21** on Sept 06, 2022, in response to evaluators' request.

<sup>71</sup>Ge Levels

E(level) <sup>†</sup>	J $\pi$	E(level) <sup>†</sup>	J $\pi$	E(level) <sup>†</sup>	J $\pi$	E(level) <sup>†</sup>	J $\pi$
0.0	1/2 <sup>-</sup>	1421.94 <sup>&amp;</sup> 13	9/2 <sup>-</sup>	3097.17 <sup>b</sup> 31	17/2 <sup>+</sup>	4472.5 <sup>c</sup> 5	23/2 <sup>-</sup>
174.9 1	5/2 <sup>-</sup>	1476.4 <sup>a</sup> 4	11/2 <sup>+</sup>	3272.26 <sup>d</sup> 19	17/2 <sup>-</sup>	4914.5 <sup>#</sup> 8	23/2 <sup>+</sup>
198.18 <sup>‡</sup> 35	9/2 <sup>+</sup>	1949.30 <sup>@</sup> 16	11/2 <sup>-</sup>	3325.06 <sup>&amp;</sup> 34	17/2 <sup>-</sup>	5009.0 <sup>‡</sup> 5	25/2 <sup>+</sup>
499.88 <sup>@</sup> 25	3/2 <sup>-</sup>	1959.1 <sup>b</sup> 4	13/2 <sup>+</sup>	3411.29 <sup>c</sup> 30	19/2 <sup>-</sup>	5274.0 <sup>d</sup> 6	25/2 <sup>-</sup>
589.5 <sup>a</sup> 4	7/2 <sup>+</sup>	2298.6 <sup>‡</sup> 4	17/2 <sup>+</sup>	3592.7 <sup>‡</sup> 4	21/2 <sup>+</sup>	5727.0 <sup>c</sup> 6	27/2 <sup>-</sup>
747.09 <sup>&amp;</sup> 23	5/2 <sup>-</sup>	2313.6 <sup>#</sup> 4	15/2 <sup>+</sup>	3599.2 <sup>#</sup> 5	19/2 <sup>+</sup>	6639.3 <sup>‡</sup> 8	29/2 <sup>+</sup>
1037.3 <sup>b</sup> 4	9/2 <sup>+</sup>	2348.85 <sup>&amp;</sup> 16	13/2 <sup>-</sup>	3757.2 <sup>@</sup> 10	(19/2 <sup>-</sup> )	7113.8 <sup>c</sup> 9	31/2 <sup>-</sup>
1096.10 <sup>@</sup> 13	7/2 <sup>-</sup>	2698.4 <sup>a</sup> 7	15/2 <sup>+</sup>	4013.3 <sup>a</sup> 10	(19/2 <sup>+</sup> )		
1172.28 <sup>‡</sup> 34	13/2 <sup>+</sup>	2836.94 <sup>c</sup> 32	15/2 <sup>-</sup>	4098.49 <sup>d</sup> 30	21/2 <sup>-</sup>		
1192.00 <sup>#</sup> 35	11/2 <sup>+</sup>	2890.23 <sup>@</sup> 29	15/2 <sup>-</sup>	4363.0 <sup>&amp;</sup> 10	(21/2 <sup>-</sup> )		

<sup>†</sup> From least-squares fit to E $\gamma$  data.

<sup>‡</sup> Band(A): Band based on 198, 9/2<sup>+</sup>,  $\alpha=+1/2$ .

<sup>#</sup> Band(a): Band based on 11/2<sup>+</sup>,  $\alpha=-1/2$ .

<sup>@</sup> Band(B): Band based on 3/2<sup>-</sup>,  $\alpha=-1/2$ .

<sup>&</sup> Band(b): Band based on 5/2<sup>-</sup>,  $\alpha=+1/2$ .

<sup>a</sup> Band(C): Band based on 7/2<sup>+</sup>,  $\alpha=-1/2$ .

<sup>b</sup> Band(c): Band based on 1038, 9/2<sup>+</sup>,  $\alpha=+1/2$ .

<sup>c</sup> Band(D): Octupole band based on 15/2<sup>-</sup>,  $\alpha=-1/2$ .

<sup>d</sup> Band(d): Octupole band based on 17/2<sup>-</sup>,  $\alpha=+1/2$ .

$\gamma(^{71}\text{Ge})$

The  $\gamma\gamma(\theta)$ (ADO) ratios are for I $\gamma$ (135°)/I $\gamma$ (90°), with typical ratios of  $\approx 1.2$  for stretched quadrupole and  $\approx 0.8$  for stretched dipole transitions.

E $\gamma$ <sup>†</sup>	I $\gamma$	E <sub>i</sub> (level)	J $\pi$ <sub>i</sub>	E <sub>f</sub>	J $\pi$ <sub>f</sub>	Mult. <sup>‡</sup>	Comments
139.1 6	1.0 2	3411.29	19/2 <sup>-</sup>	3272.26	17/2 <sup>-</sup>	(D)	R <sub>ADO</sub> =0.89 28.
174.9 1	75 11	174.9	5/2 <sup>-</sup>	0.0	1/2 <sup>-</sup>	(Q)	R <sub>ADO</sub> =1.13 23.
247.3 6	4.1 7	747.09	5/2 <sup>-</sup>	499.88	3/2 <sup>-</sup>	(D)	R <sub>ADO</sub> =0.93 15.
314.1 1	16.7 26	3411.29	19/2 <sup>-</sup>	3097.17	17/2 <sup>+</sup>	E1	R <sub>ADO</sub> =0.78 12; POL=+0.21 8.
326.1 6	2.0 3	1421.94	9/2 <sup>-</sup>	1096.10	7/2 <sup>-</sup>	D	R <sub>ADO</sub> =0.81 16.
349.0 6	1.2 2	1096.10	7/2 <sup>-</sup>	747.09	5/2 <sup>-</sup>	D	R <sub>ADO</sub> =0.82 15.
373.9 6	3.9 6	4472.5	23/2 <sup>-</sup>	4098.49	21/2 <sup>-</sup>	D	R <sub>ADO</sub> =0.83 12.
391.3 1	15.6 25	589.5	7/2 <sup>+</sup>	198.18	9/2 <sup>+</sup>	M1	R <sub>ADO</sub> =0.95 15; POL=-0.33 8.
399.4 6	1.5 3	2348.85	13/2 <sup>-</sup>	1949.30	11/2 <sup>-</sup>	D	R <sub>ADO</sub> =0.53 8.

Continued on next page (footnotes at end of table)

<sup>74</sup>Ge( $\alpha,\alpha 3n\gamma$ ) 2022Wa21 (continued)

$\gamma(^{71}\text{Ge})$  (continued)

$E_\gamma$ †	$I_\gamma$	$E_i$ (level)	$J_i^\pi$	$E_f$	$J_f^\pi$	Mult. ‡	Comments
435.3 6	1.3 2	3272.26	17/2 <sup>-</sup>	2836.94	15/2 <sup>-</sup>	D	RADO=0.72 11.
447.9 3	5.4 8	1037.3	9/2 <sup>+</sup>	589.5	7/2 <sup>+</sup>	M1+E2	RADO=1.04 14; POL=-0.35 14.
453.0 6	1.5 3	5727.0	27/2 <sup>-</sup>	5274.0	25/2 <sup>-</sup>	D	RADO=0.52 7.
482.6 6	4.3 6	1959.1	13/2 <sup>+</sup>	1476.4	11/2 <sup>+</sup>	D	RADO=0.90 11.
499.9 3	7.6 10	499.88	3/2 <sup>-</sup>	0.0	1/2 <sup>-</sup>		RADO=1.15 13.
521.1 6	3.1 6	3411.29	19/2 <sup>-</sup>	2890.23	15/2 <sup>-</sup>	(Q)	RADO=1.65 18.
527.2 6	1.7 3	1949.30	11/2 <sup>-</sup>	1421.94	9/2 <sup>-</sup>	D	RADO=0.58 5.
541.1 6	1.2 2	2890.23	15/2 <sup>-</sup>	2348.85	13/2 <sup>-</sup>	D	RADO=0.56 6.
572.1 6	3.5 6	747.09	5/2 <sup>-</sup>	174.9	5/2 <sup>-</sup>	D	RADO=1.09 10; $\Delta J=0$ transition.
574.4 3	9.4 13	3411.29	19/2 <sup>-</sup>	2836.94	15/2 <sup>-</sup>	E2	RADO=1.50 13; POL=+0.41 9.
596.2 6	4.1 7	1096.10	7/2 <sup>-</sup>	499.88	3/2 <sup>-</sup>	Q	RADO=1.40 12.
674.9 3	8.1 10	1421.94	9/2 <sup>-</sup>	747.09	5/2 <sup>-</sup>	Q	RADO=1.25 9.
687.2 3	5.6 4	4098.49	21/2 <sup>-</sup>	3411.29	19/2 <sup>-</sup>	M1	RADO=0.81 6; POL=-0.33 11.
747.3 6	2.1 4	747.09	5/2 <sup>-</sup>	0.0	1/2 <sup>-</sup>	Q	RADO=1.25 8.
767.1 3	5.8 10	1959.1	13/2 <sup>+</sup>	1192.00	11/2 <sup>+</sup>	D+Q	RADO=1.36 9.
783.4 3	13.2 15	3097.17	17/2 <sup>+</sup>	2313.6	15/2 <sup>+</sup>	M1	RADO=0.85 5; POL=-0.41 9.
786.9 6	4.1 6	1959.1	13/2 <sup>+</sup>	1172.28	13/2 <sup>+</sup>	D+Q	RADO=0.73 6; $\Delta J=0$ transition.
798.8 6	1.5 3	3097.17	17/2 <sup>+</sup>	2298.6	17/2 <sup>+</sup>	D	RADO=1.07 10; $\Delta J=0$ transition.
826.2 3	9.0 10	4098.49	21/2 <sup>-</sup>	3272.26	17/2 <sup>-</sup>	E2	RADO=1.43 12; POL=+0.52 12.
839.0 3	10.5 20	1037.3	9/2 <sup>+</sup>	198.18	9/2 <sup>+</sup>	D	RADO=1.22 7; $\Delta J=0$ transition.
853.2 1	17.5 25	1949.30	11/2 <sup>-</sup>	1096.10	7/2 <sup>-</sup>	E2	RADO=1.29 6; POL=+0.49 12.
867.0		3757.2	(19/2 <sup>-</sup> )	2890.23	15/2 <sup>-</sup>		
877.8 6	3.0 6	2836.94	15/2 <sup>-</sup>	1959.1	13/2 <sup>+</sup>	D	RADO=0.68 17.
887.0 3	8.4 15	1476.4	11/2 <sup>+</sup>	589.5	7/2 <sup>+</sup>	E2	RADO=1.20 7; POL=+0.23 14.
887.6 6	2.2 4	2836.94	15/2 <sup>-</sup>	1949.30	11/2 <sup>-</sup>	Q	RADO=1.43 9.
921.2 1	19.7 26	1096.10	7/2 <sup>-</sup>	174.9	5/2 <sup>-</sup>	M1	RADO=0.67 3; POL=-0.32 9.
921.8 6	1.5 3	1959.1	13/2 <sup>+</sup>	1037.3	9/2 <sup>+</sup>	Q	RADO=1.27 10.
923.4 1	21.8 26	3272.26	17/2 <sup>-</sup>	2348.85	13/2 <sup>-</sup>	E2	RADO=1.28 9; POL=+0.43 9.
926.9 1	39.8 52	2348.85	13/2 <sup>-</sup>	1421.94	9/2 <sup>-</sup>	E2	RADO=1.27 9; POL=+0.33 13.
941.0 3	9.6 11	2890.23	15/2 <sup>-</sup>	1949.30	11/2 <sup>-</sup>	E2	RADO=1.18 6; POL=+0.38 12.
974.1 1	100.0	1172.28	13/2 <sup>+</sup>	198.18	9/2 <sup>+</sup>	E2	RADO=1.31 7; POL=+0.53 16.
976.2 3	6.4 9	3325.06	17/2 <sup>-</sup>	2348.85	13/2 <sup>-</sup>	E2	RADO=1.12 12; POL=+0.44 18.
993.8 1	53.2 56	1192.00	11/2 <sup>+</sup>	198.18	9/2 <sup>+</sup>	M1+E2	RADO=1.34 7; POL=-0.21 13.
1037.9#		4363.0?	(21/2 <sup>-</sup> )	3325.06	17/2 <sup>-</sup>		
1061.3 6	1.5 4	4472.5	23/2 <sup>-</sup>	3411.29	19/2 <sup>-</sup>	Q	RADO=1.19 14.
1113.1 6	3.0 5	3411.29	19/2 <sup>-</sup>	2298.6	17/2 <sup>+</sup>	D	RADO=0.57 10.
1121.6 1	26.4 32	2313.6	15/2 <sup>+</sup>	1192.00	11/2 <sup>+</sup>	E2	RADO=1.16 6; POL=+0.42 16.
1126.3 1	45.1 62	2298.6	17/2 <sup>+</sup>	1172.28	13/2 <sup>+</sup>	E2	RADO=1.22 6; POL=+0.52 9.
1138.1 3	13.2 14	3097.17	17/2 <sup>+</sup>	1959.1	13/2 <sup>+</sup>	E2	RADO=1.23 9; POL=+0.33 22.
1141.3 6	2.4 4	2313.6	15/2 <sup>+</sup>	1172.28	13/2 <sup>+</sup>	D+Q	RADO=1.14 7.
1175.6 6	1.5 3	5274.0	25/2 <sup>-</sup>	4098.49	21/2 <sup>-</sup>	Q	RADO=1.36 11.
1222.0 6	2.4 4	2698.4	15/2 <sup>+</sup>	1476.4	11/2 <sup>+</sup>	(Q)	RADO=1.52 12.
1247.0 1	51.7 60	1421.94	9/2 <sup>-</sup>	174.9	5/2 <sup>-</sup>	E2	RADO=1.30 8; POL=+0.42 13.
1254.4 6	2.8 5	5727.0	27/2 <sup>-</sup>	4472.5	23/2 <sup>-</sup>	Q	RADO=1.31 9.
1278.1 3	8.9 15	1476.4	11/2 <sup>+</sup>	198.18	9/2 <sup>+</sup>	D	RADO=1.01 11.
1285.6 3	8.2 10	3599.2	19/2 <sup>+</sup>	2313.6	15/2 <sup>+</sup>	Q	RADO=1.26 8.
1294.1 1	22.7 15	3592.7	21/2 <sup>+</sup>	2298.6	17/2 <sup>+</sup>	E2	RADO=1.31 7; POL=+0.32 14.
1314.9#		4013.3?	(19/2 <sup>+</sup> )	2698.4	15/2 <sup>+</sup>		
1315.2 6	1.9 3	4914.5	23/2 <sup>+</sup>	3599.2	19/2 <sup>+</sup>	Q	RADO=1.21 9.
1386.8 6	1.5 3	7113.8	31/2 <sup>-</sup>	5727.0	27/2 <sup>-</sup>	Q	RADO=1.16 9.
1416.3 3	7.3 7	5009.0	25/2 <sup>+</sup>	3592.7	21/2 <sup>+</sup>	Q	RADO=1.40 10.
1630.3 6	1.3 2	6639.3	29/2 <sup>+</sup>	5009.0	25/2 <sup>+</sup>	Q	RADO=1.49 17.
1664.7 3	12.7 17	2836.94	15/2 <sup>-</sup>	1172.28	13/2 <sup>+</sup>	E1	RADO=0.79 7; POL=+0.34 16.
1760.9 6	2.1 4	1959.1	13/2 <sup>+</sup>	198.18	9/2 <sup>+</sup>	Q	RADO=1.18 13.
1924.5 6	0.4 1	3097.17	17/2 <sup>+</sup>	1172.28	13/2 <sup>+</sup>		

Continued on next page (footnotes at end of table)

---

 ${}^{74}\text{Ge}(\alpha, \alpha 3n\gamma)$  **2022Wa21 (continued)**

---

 $\gamma({}^{71}\text{Ge})$  (continued)

† Uncertainties are stated as 0.1-0.6 keV by authors in their Sept 06, 2022 communication. Evaluators assign 0.1 keV for  $E_\gamma$  values with  $I_\gamma \geq 15$ , 0.3 keV for  $I_\gamma = 5-15$ , and 0.6 keV for  $I_\gamma \leq 5$ .

‡ Assigned by evaluators from  $R_{\text{ADO}}$  and linear polarization in [2022Wa21](#). Mult=Q is most likely E2.

# Placement of transition in the level scheme is uncertain.

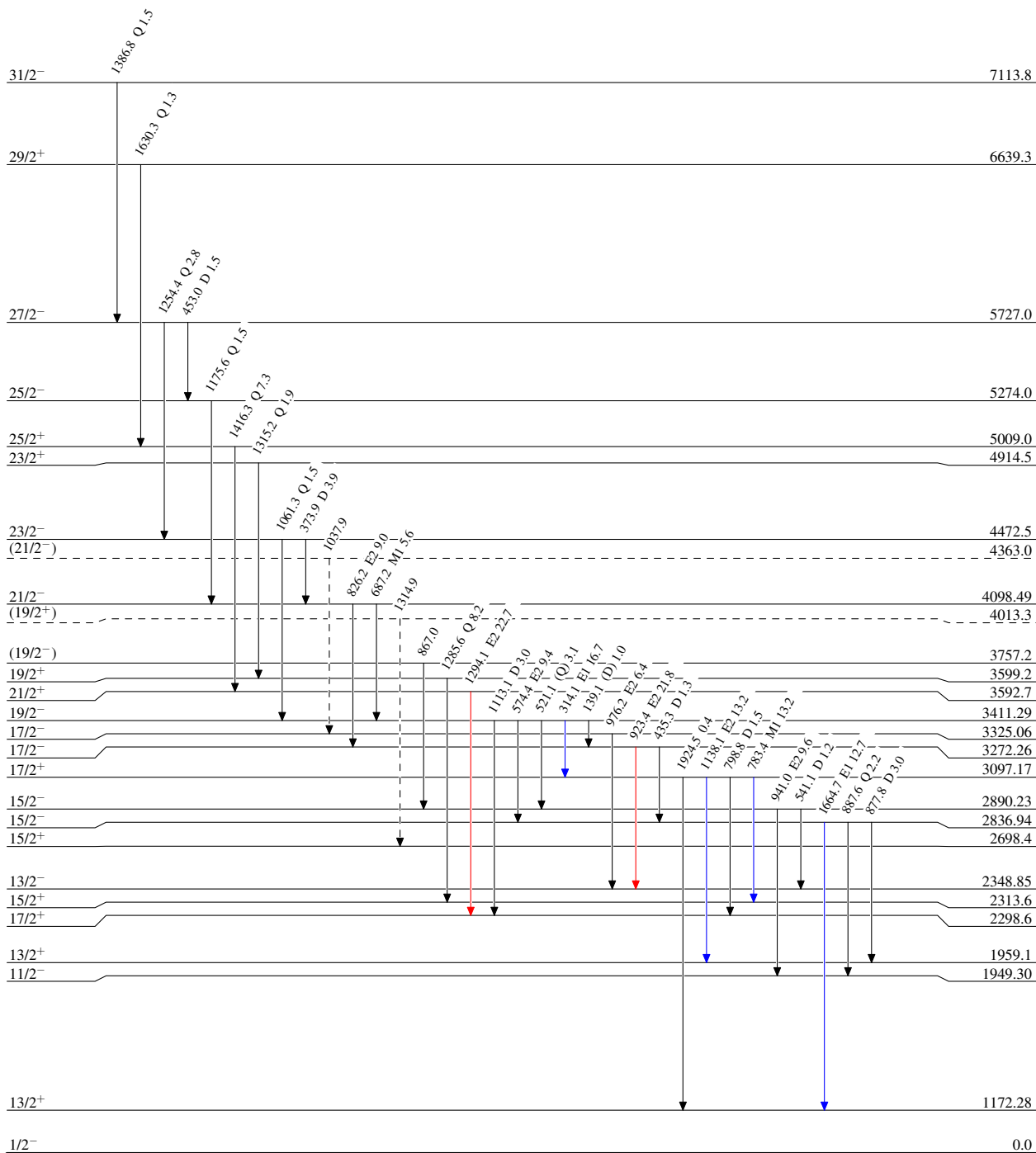
<sup>74</sup>Ge( $\alpha, \alpha 3n\gamma$ ) 2022Wa21

Legend

Level Scheme

Intensities: Relative I<sub>γ</sub>

- I<sub>γ</sub> < 2% × I<sub>γ</sub><sup>max</sup>
- I<sub>γ</sub> < 10% × I<sub>γ</sub><sup>max</sup>
- I<sub>γ</sub> > 10% × I<sub>γ</sub><sup>max</sup>
- - - - -→ γ Decay (Uncertain)



<sup>71</sup>Ge<sub>39</sub>

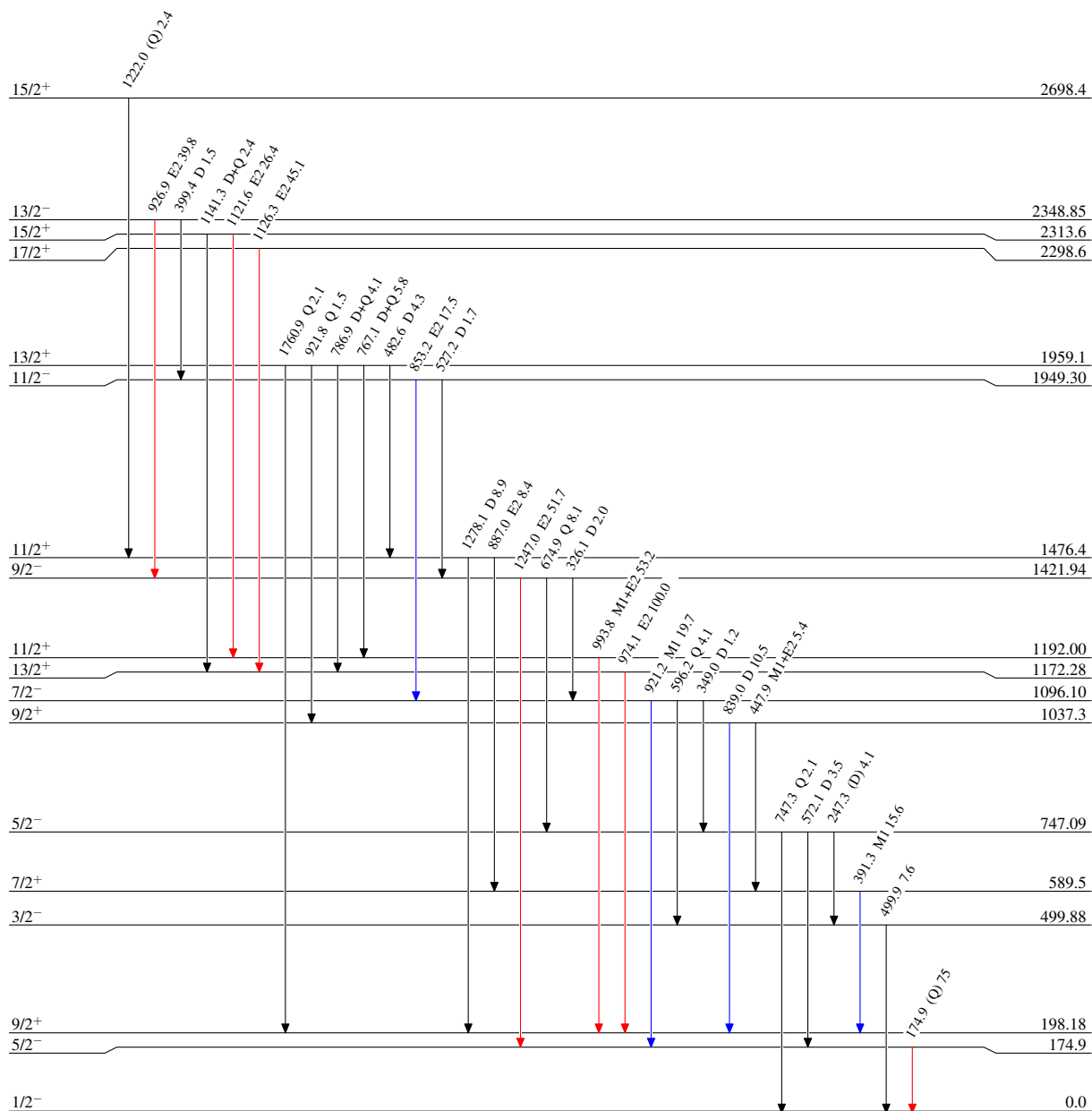
$^{74}\text{Ge}(\alpha,\alpha 3n\gamma)$  2022Wa21

Level Scheme (continued)

Intensities: Relative  $I_\gamma$

Legend

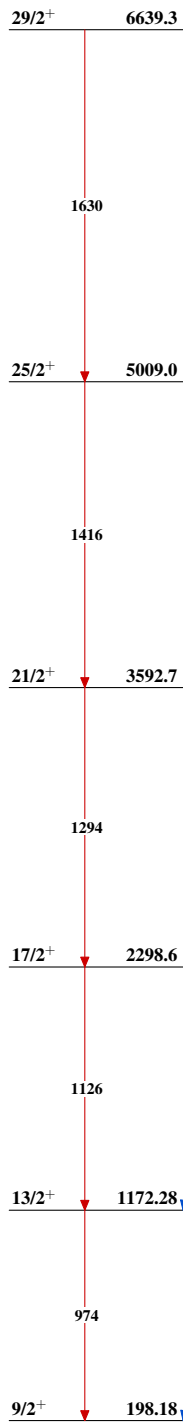
- $I_\gamma < 2\% \times I_\gamma^{\max}$
- $I_\gamma < 10\% \times I_\gamma^{\max}$
- $I_\gamma > 10\% \times I_\gamma^{\max}$



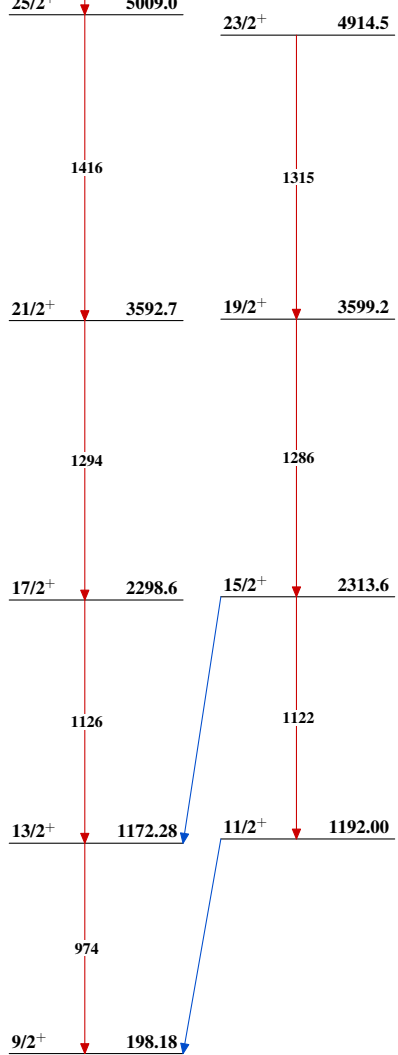
$^{71}_{32}\text{Ge}_{39}$

${}^{74}\text{Ge}(\alpha, \alpha 3n\gamma)$  2022Wa21

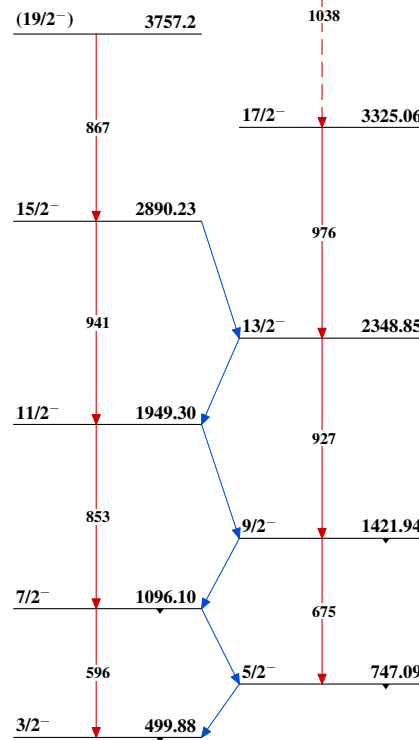
Band(A): Band based on  
198,  $9/2^+$ ,  $\alpha=+1/2$



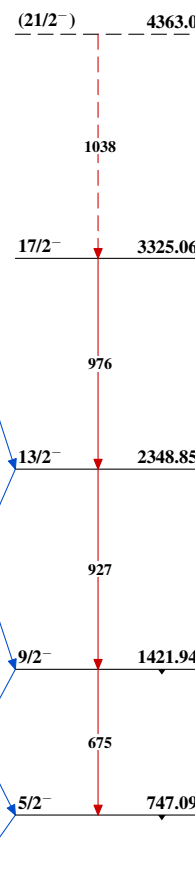
Band(a): Band based on  
 $11/2^+$ ,  $\alpha=-1/2$



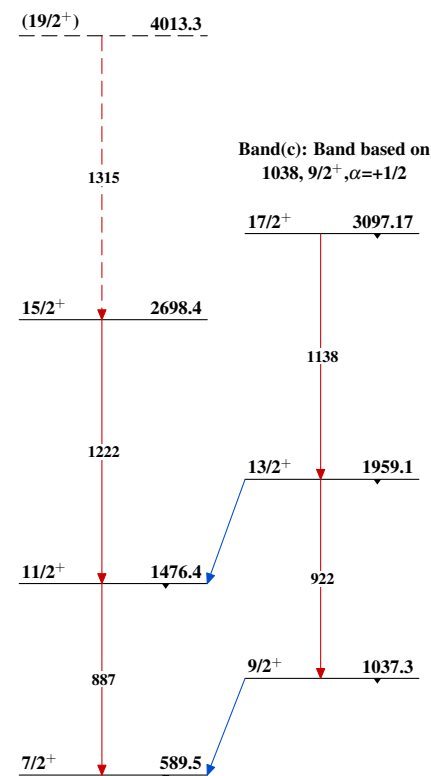
Band(B): Band based on  
 $3/2^-$ ,  $\alpha=-1/2$



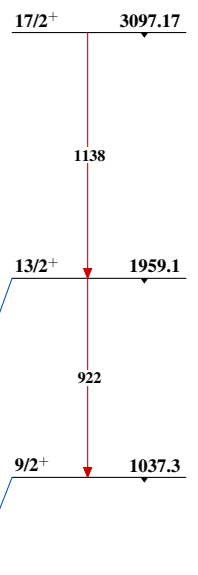
Band(b): Band based on  
 $5/2^-$ ,  $\alpha=+1/2$



Band(C): Band based on  
 $7/2^+$ ,  $\alpha=-1/2$

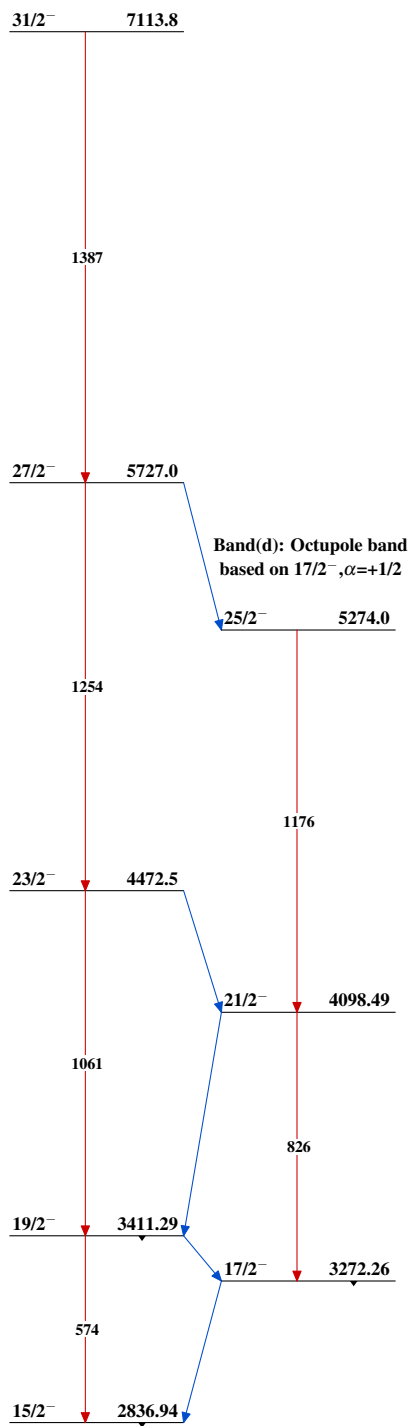


Band(c): Band based on  
1038,  $9/2^+$ ,  $\alpha=+1/2$

 ${}^{71}_{32}\text{Ge}_{39}$

$^{74}\text{Ge}(\alpha, \alpha 3n\gamma)$  2022Wa21 (continued)

Band(D): Octupole band  
based on  $15/2^{-}, \alpha=-1/2$

 $^{71}_{32}\text{Ge}_{39}$